Demonstration of a Stable Atom-Photon Entanglement Source for Quantum Repeaters

Shuai Chen,[1] Yu-Ao Chen,[1] Bo Zhao,[1] Zhen-Sheng Yuan,[1,2] Jörg Schmiedmayer,[3,1] and Jian-Wei Pan[1,2]

[1]*Physikalisches Institut, Ruprecht-Karls-Universität Heidelberg, Philosophenweg 12, 69120 Heidelberg, Germany*

[2]*Hefei National Laboratory for Physical Sciences at Microscale and Department of Modern Physics, University of Science and Technology of China, Hefei, Anhui 230026, China*

[3]*Atominstitut der österreichischen Universitäten, TU-Wien, A-1020 Vienna Austria*

(Received 15 June 2007; published 2 November 2007)

We demonstrate a novel way to efficiently create a robust entanglement between an atomic and a photonic qubit. A single laser beam is used to excite one atomic ensemble and two different modes of Raman fields are collected to generate the atom-photon entanglement. With the help of built-in quantum memory, the entanglement still exists after 20.5 μs storage time which is further proved by the violation of Clauser-Horne-Shimony-Holt type Bell's inequality. The entanglement procedure can serve as a building block for a novel robust quantum repeater architecture [Zhao *et al.*, Phys. Rev. Lett. **98**, 240502 (2007)] and can be extended to generate high-dimensional atom-photon entanglements.

DOI: 10.1103/PhysRevLett.99.180505 PACS numbers: 03.67.Hk, 32.80.Pj, 42.50.Dv

Quantum communication provides an absolutely secure approach to transfer information. Unfortunately, the photon transmission loss and the decoherence which scale exponentially with the length of the communication channel make it extremely hard to deliver quantum information over long distances effectively. A quantum repeater protocol [1] combining the entanglement swapping, purification and quantum memory provides a remarkable way to establish high-quality long-distance quantum networks, and makes the communicating resources increase only polynomially with transmission distance.

Following a scheme proposed by Duan, Lukin, Cirac, and Zoller (DLCZ) [2], in recent years, significant experimental advances have been achieved towards the implementation of the quantum repeater protocol by using the atomic ensemble and linear optics [3–9]. However, the DLCZ protocol has an inherent drawback which is severe enough to make a long-distance quantum communication extremely difficult [10,11]. The phase fluctuation caused by path length instability over long distance is very hard to overcome. Recently, a more robust quantum repeater architecture was proposed to bypass the phase fluctuation over long distance [10,11]. This architecture is insensitive to the relative phase between two photons. Several experiments have proven that the path length fluctuations only need to be kept on the scale of the photon's coherent length, from hundreds of micrometer [12] to tens of meters [13–15]. In the original protocol [10,11], two laser beams with fixed relative phase are used to excite two atomic ensembles to generate the atom-photon entanglement for the local communication node. Only the path length between two ensembles in the local node need to be stabilized to subwavelength scale. Some recent progresses provided various techniques to generate atom-photon entanglement, including spin excitation of magnetic sublevels [16,17] and dual-species atomic ensemble [18]. But the remaining problems like balancing of the excitations between magnetic sublevels and efficiency of frequency mixing limits the further application. Another kind of atom-photon entanglement is realized using the orbital angular momentum (OAM) states [19], which could also extend to high-dimensional entanglement. However, the divergence property of different OAM modes makes it impractical for long-distance quantum communication [20].

In this Letter, we present a new approach to effectively generate the entanglement between the atomic qubit and photonic qubit based on atomic ensemble in a local magneto-optical trap (MOT). It satisfies the requirements of the improved protocol [10]. In contrast with previous experiments [6,7,16–19], the atomic ensemble is excited by only one write beam with single frequency, while two spontaneous Raman scattered fields (anti-Stokes fields) in different spatial modes are combined on a polarizing beam splitter (PBS) to serve as the photonic qubit. The corresponding collective spin excitations in the atomic ensemble represent the atomic qubit. Moreover, the relative phase difference between the two selected modes is actively stabilized by the local build-in Mach-Zehnder interferometer [21] to prevent for the phase drift. Based on the character of the spatial modes we selected, our approach is suitable to perform long-distance quantum communication. Besides, by extending the approach to select more spatial modes of collective excitation, high-dimensional entanglement state could be easily realized.

The basic setup of our experiment is shown in Fig. 1. A cold ^{87}Rb atomic cloud with temperature about 100 μK in the MOT is worked as the medium to generate and store the information of the quantum excitation. The two hyperfine ground states $|5S_{1/2}, F = 2\rangle = |a\rangle$ and $|5S_{1/2}, F = 1\rangle = |b\rangle$ and the excited state $|5P_{1/2}, F = 2\rangle = |e\rangle$ form a Λ-type system. After loading the MOT, the atoms are first pumped to initial state $|a\rangle$. A single weak 75 ns write beam illuminates the atom cloud with beam waist of 240 μm and 10 MHz red-detuned to $|a\rangle \rightarrow |e\rangle$ transition. Two anti-

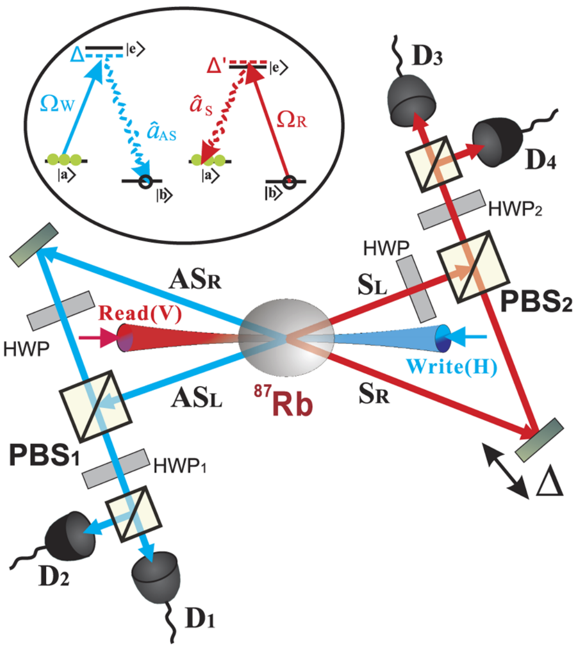

FIG. 1 (color online). Illustration of the scheme of the experiment setup and the relevant energy levels of the ^{87}Rb atoms. Cold ^{87}Rb atoms captured by MOT are initially prepared in state $|a\rangle$. A weak horizontal polarized write pulse Ω_W illuminates the atom cloud. The spontaneous Raman scattered anti-Stokes field AS_L and AS_R with vertical polarization are collected at $\pm 3°$ to the propagating direction of the write beam, defining the spatial mode of the atomic ensembles L and R, respectively. The AS_R mode is rotated to be horizontal polarized, combined with AS_L mode on a polarizing beam splitter PBS_1 and sent to the polarization analyzer. This creates the entanglement between the polarization of the anti-Stokes field and the spatial modes of spin excitation in the atomic ensemble. To verify the entanglement after a storage time τ, a vertical polarized read pulse counter-propagating with write pulse is applied to retrieve the spin excitation to the Stokes fields S_L and S_R. The polarization of S_L is rotated by 90°, combined with S_R on PBS_2 and sent to the polarization analyzer.

Stokes fields ($|e\rangle \rightarrow |b\rangle$, Laguerre-Gauss LG_{00} mode, 70 μm waist) AS_L and AS_R induced by the write beam via spontaneous Raman scattering are collected at $\pm 3°$ relative to the propagating direction of the write beam. This also defines the spatial mode of the atomic ensemble L and R. With small excitation probability, the atom-light field can be expressed as [2]

$$|\Psi\rangle_m \sim |0_{\mathrm{AS}} 0_b\rangle_m + \sqrt{\chi_m} |1_{\mathrm{AS}} 1_b\rangle_m + O(\chi_m), \quad (1)$$

where $\chi_m \ll 1$ is the excitation probability of one collective spin in ensemble m ($m = L, R$), and $\sqrt{\chi_m} |i_{\mathrm{AS}} i_b\rangle_m$ denote the i-fold excitation of the anti-Stokes light field and the collective spin in atomic ensemble.

Because of the momentum conservation, the overall k vector of the collective excitation after the spontaneous Raman scattering is $\vec{k}_{\mathrm{atom}} = \vec{k}_W - \vec{k}_{\mathrm{AS}}$, where $\vec{k}_{\mathrm{AS}}$ and $\vec{k}_W$ are the wave vector of the anti-Stokes field and write beam, respectively. If no external field interrupts the atomic state during the storage time τ, $\vec{k}_{\mathrm{atom}}$ is kept. When the read pulse is applied to retrieve the collective excitation into a correlated Stokes field, $\vec{k}_{\mathrm{atom}}$ is transferred to the Stokes field. The wave vector of the Stokes field becomes $\vec{k}_S = \vec{k}_R + \vec{k}_{\mathrm{atom}}$, where $\vec{k}_R$ represents the wave vector of the read beam [22]. Then we have

$$\vec{k}_S = \vec{k}_R + \vec{k}_W - \vec{k}_{\mathrm{AS}}. \quad (2)$$

Under the counterpropagating condition of read and write beams (shown in Fig. 1), $\vec{k}_S \simeq -\vec{k}_{\mathrm{AS}}$.

To characterize the light field, we measure the cross correlation $g^{(2)}_{\mathrm{AS},S}$ [3,8], which marks the degree of quantum correlation, between the anti-Stokes and the Stokes fields. As two anti-Stokes fields AS_L and AS_R are detected at two different spatial modes, two corresponding Stokes fields S_L and S_R can be detected during the retrieve process. For the mode-matched fields S_L and AS_L (S_R and AS_R), the cross correlation $g^{(2)}_{\mathrm{AS},S} \gg 1$ when $\chi \ll 1$, which means good quantum correlation between those fields. But for the unmatched fields S_L and AS_R (S_R and AS_L), no quantum correlation is observed ($g^{(2)}_{\mathrm{AS},S} \sim 1$). The cross-talk between these two different modes is negligible. The viability of our new approach is guaranteed by this condition.

We adjust the two modes L and R to be equal excited ($\chi_L = \chi_R = \chi$). The two anti-Stokes fields are combined on PBS_1 and sent into a polarization analyzer, as illustrated in Fig. 1. Neglecting the vacuum state and high order excitations, the entangled states between the photonic and the atomic qubit can be described as

$$|\Psi\rangle = \frac{1}{\sqrt{2}} (|H\rangle|R\rangle + e^{i\phi_1}|V\rangle|L\rangle), \quad (3)$$

where $|H\rangle/|V\rangle$ denotes horizontal (vertical) polarizations of the single anti-Stokes photon and $|L\rangle/|R\rangle$ denotes single collective spin excitation in ensemble L/R, ϕ_1 is the propagating phase difference between the two anti-Stokes fields before they overlap at PBS_1. Physically, the atom-photon entangled state (3) is equivalent to the maximally polarization entangled state generated by spontaneous parametric down-conversion [23].

To verify the entanglement between the anti-Stokes field and the atomic spin excitation, a relative strong read pulse with 75 ns close to resonance of $|e\rangle \rightarrow |b\rangle$ transition counter-propagating with the write beam is applied after a controllable time τ to convert the atomic collective spin excitation back into Stokes fields.

After combine the two Stokes fields on PBS_2 (see Fig. 1), the superposition state of anti-Stokes and Stokes fields is the following maximally polarization entangled state

$$|\Psi\rangle_{AS,S} = \frac{1}{\sqrt{2}}(|H\rangle_{AS}|H\rangle_S + e^{i(\phi_1+\phi_2)}|V\rangle_{AS}|V\rangle_S), \quad (4)$$

where ϕ_2 represent the propagating phase difference between two Stokes fields before they overlap at the PBS_2. In our experiment, the total phase $\phi_1 + \phi_2$ is actively stabilized via the built-in Mach-Zehnder interferometer and fixed to zero [21]. After the stabilization, the short term phase fluctuation is smaller than $\pi/30$ and long term drift is cancelled, which guarantees the stability of our experiment.

To investigate the scaling of entanglement with the excitation probability χ, we measure the visibility V of the interference fringes of the coincidence rate between anti-Stokes and Stokes photons for various value of χ with fixed memory time $\tau = 500$ ns. The half wave plate HWP_1 (see Fig. 1) is set to $+22.5°$ to measure the anti-Stokes fields under $|H\rangle + |V\rangle$ base and rotate HWP_2 to measure the Stokes fields under different bases. As χ increases, the high order term in Eq. (1) cannot be neglected. The visibility V can be expressed as the function of cross correlation between the anti-Stokes and Stokes fields [17]

$$V = \frac{g^{(2)}_{AS,S} - 1}{g^{(2)}_{AS,S} + 1}. \quad (5)$$

Ideally, the relationship of the excitation rate χ and cross correlation $g^{(2)}_{AS,S}$ is $g^{(2)}_{AS,S} = 1 + 1/\chi$ at low excitation limit ($\chi \ll 1$). Considering the detected efficiency of the anti-Stokes field η_{AS}, we have the detection rate of the anti-Stokes photon $p_{AS} = \eta_{AS}\chi$. The visibility can be expressed as

$$V = 1 - 2p_{AS}/\eta_{AS}. \quad (6)$$

In our experiment, $\eta_{AS} \sim 8\%$. Figure 2 shows the measured visibility V varying with p_{AS}. As the excitation rate χ decrease, which corresponds to decrease of p_{AS}, the visibility V increases as does the degree of entanglement. The solid line is the linear fit for the experiment data. At $p_{AS} \to 0$, V is near 0.95. This imperfection is mainly caused by the overlap of the two anti-Stokes fields AS_L and AS_R, the noise of the detector and the phase fluctuation in the interferometer. As the detection rate p_{AS} increases, the probability of high order excitations increases faster than that of the single excitation. Then the correlation $g^{(2)}_{AS}$ decreases, as well as the visibility. At $p_{AS} < 1.3 \times 10^{-2}$, V is larger than $1/\sqrt{2}$ which marks the bound of violation of the Clauser-Horne-Shimony-Holt (CHSH) type Bell's inequality [17,24]. All the error bars presented in the figures in this letter show the statistical error, which is the Poissonian propagation from the square root of the counts.

To further study the storage ability of the atomic ensemble quantum memory, we characterize the temporal decay of entanglement with storage time τ. Here we measure the decay of the S parameter, sum of the correlation function in CHSH-type Bell's inequality, where $S \leq 2$ for any local realistic theory with

$$S = |E(\theta_1, \theta_2) - E(\theta_1, \theta_2') - E(\theta_1', \theta_2) - E(\theta_1', \theta_2')|. \quad (7)$$

Here $E(\theta_1, \theta_2)$ is the correlation function, where θ_1 and θ_2' (θ_1' and θ_2') are the measured polarization bases of the anti-Stokes field and Stokes field. During the measurement, the HWP_1 and HWP_2 are set to different angles to make the bases settings at (0°,22.5°), (0°, − 22.5°), (45°,22.5°) and (45°, − 22.5°), respectively. The excitation rate χ was fixed to get $p_{AS} = 2 \times 10^{-3}$, and the result of measurement is shown in Fig. 3. At the storage time of 500 ns, $S = 2.60 \pm 0.03$, which violates Bell's inequality by 20 stan-

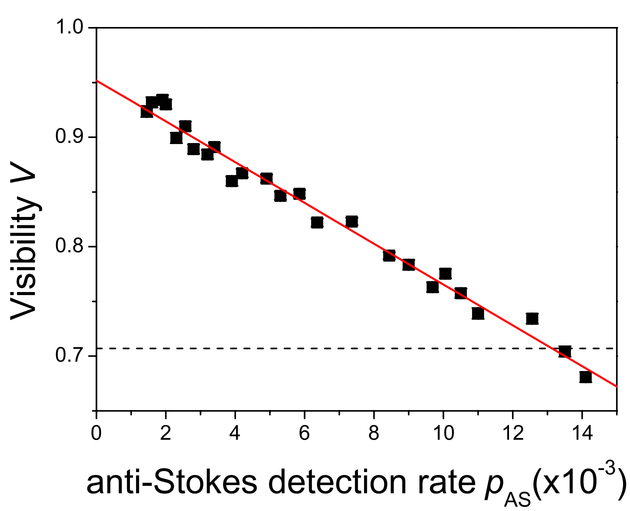

FIG. 2 (color online). Visibility of the interference fringes V between Anti-Stokes fields and Stokes fields various with anti-Stokes detecting rate p_{AS}. The solid line is the fit corresponding to Eq. (6). The dashed line shows the bound of $1/\sqrt{2}$ which mark the limit to violate the CHSH-type Bell's inequality.

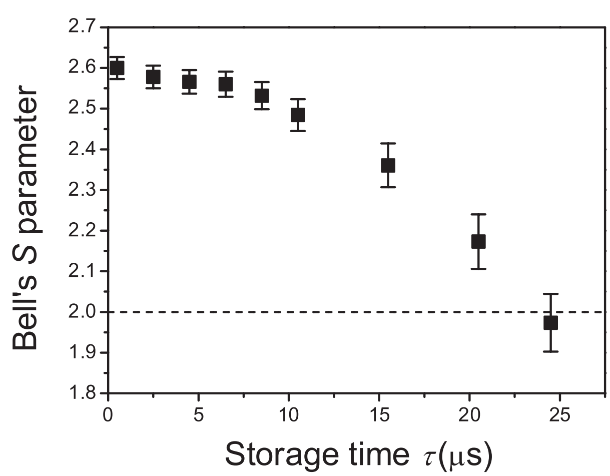

FIG. 3. Decay of the S parameter in the Bell's inequality measurement with the storage time τ. The dashed line shows the classical bound of $S = 2$.

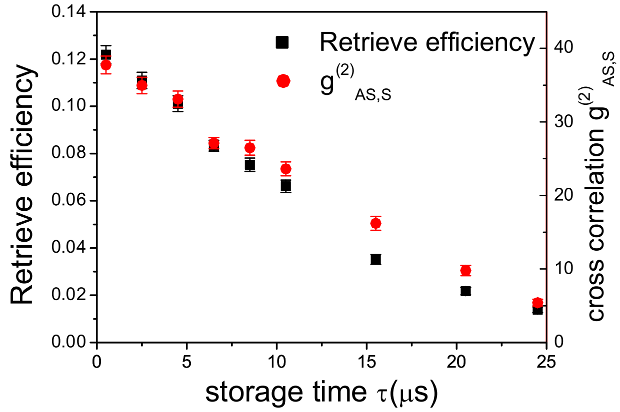

FIG. 4 (color online). The decay of retrieve efficiency and cross correlation $g^{(2)}_{\mathrm{AS},S}$ with the storage time τ. The anti-Stokes detection rate is fixed at $p_{\mathrm{AS}} = 2 \times 10^{-3}$. The square dots show the decay process of the retrieve efficiency of the Stokes fields, round dots show the decay of the cross correlation $g^{(2)}_{\mathrm{AS},S}$ between anti-Stokes field and Stokes field.

dard deviations. As the storage time increases, the S parameter decreases, indicating the decoherence of the entanglement. At storage time $\tau = 20.5$ μs, we still get $S = 2.17 \pm 0.07$, which means the character of quantum entanglement is still well preserved. The decay of S parameter with increasing storage time τ is caused by the residual magnetic field which inhomogeneously broadens the ground state magnetic sublevels. This process can be observed from the decay of the retrieve efficiency and the cross correlation between anti-Stokes and Stokes fields.

Shown in Fig. 4, the retrieve efficiency and the cross correlation between anti-Stokes and Stokes field all decreases with increasing the storage time τ. At $\tau = 500$ ns, the overall retrieve efficiency (coincidence counts of Stokes and anti-Stokes photons over the counts of anti-Stokes photons, including the transmission loss and the detector efficiency) is $12.2 \pm 0.4\%$ and the cross correlation $g^{(2)}_{\mathrm{AS},S} = 38 \pm 1$. At $\tau = 20.5$ μs, the retrieve efficiency and cross correlation decrease to $2.2 \pm 0.1\%$ and $g^{(2)}_{\mathrm{AS},S} = 9.8 \pm 0.7$, respectively. These values are still sufficient to violate the CHSH-type Bell's inequality. When τ is longer than 24 μs, $g^{(2)}_{\mathrm{AS},S} < 6$ makes it insufficient to violate the Bell's inequality.

In conclusion, we have generated a stable atom-photon entanglement with a novel approach. A single write beam and a single atomic ensemble are used to generate the collective spin excitations. Two spatial modes of collective excitations are defined by the collection modes of anti-Stokes fields. The conservation of momentum during the atom-photon interaction prevent for the cross talk between different excited spatial modes. The visibility of the entanglement and violation of the CHSH-type Bell's inequality are measured to prove the atom-photon entanglement between anti-Stokes photon and collective excitation in atomic ensemble. Also with the help of the build-in quantum memory, the violation of the Bell's inequality still exists after 20.5 μs, corresponding to the time of light propagating 4 km in an optical fiber. That means we have successfully achieved a memory build-in atom-photon entanglement source which can work as a node of the long-distance quantum communication networks. Furthermore, if the atomic ensemble is confined in the optical trap and "clock states" [25] is implemented, the memory time could be extended to longer than 1 ms. Moreover, if more anti-Stokes modes are selected at different angles corresponding to the write beam, this approach can be easily extended to generate high order entanglement, which could be very useful in the complex quantum cryptography and quantum computation.

This work was supported by the Deutsche Forschungsgemeinschaft (DFG), the Alexander von Humboldt Foundation, the Marie Curie Excellence Grant of the EU, the Deutsche Telekom Stiftung and the CAS.

[1] H.-J. Briegel, W. Dür, J. I. Cirac, and P. Zoller, Phys. Rev. Lett. **81**, 5932 (1998).
[2] L.-M. Duan, M. D. Lukin, J. I. Cirac, and P. Zoller, Nature (London) **414**, 413 (2001).
[3] A. Kuzmich *et al.*, Nature (London) **423**, 731 (2003).
[4] T. Chanelière *et al.*, Nature (London) **438**, 833 (2005).
[5] M. D. Eisaman *et al.*, Nature (London) **438**, 837 (2005).
[6] D. N. Matsukevich and A. Kuzmich, Science **306**, 663 (2004).
[7] C. W. Chou *et al.*, Nature (London) **438**, 828 (2005).
[8] S. Chen *et al.*, Phys. Rev. Lett. **97**, 173004 (2006).
[9] C. W. Chou *et al.*, Science 316, 1316 (2007).
[10] B. Zhao *et al.*, Phys. Rev. Lett. **98**, 240502 (2007).
[11] Z. B. Chen *et al.*, Phys. Rev. A **76**, 022329 (2007).
[12] T. Yang *et al.*, Phys. Rev. Lett. **96**, 110501 (2006).
[13] D. Felinto *et al.*, Nature Phys. **2**, 844 (2006).
[14] T. Chanelière *et al.*, Phys. Rev. Lett. **98**, 113602 (2007).
[15] Z. -S. Yuan *et al.*, Phys. Rev. Lett. **98**, 180503 (2007).
[16] D. N. Matsukevich *et al.*, Phys. Rev. Lett. **95**, 040405 (2005).
[17] H. de Riedmatten *et al.*, Phys. Rev. Lett. **97**, 113603 (2006).
[18] S.-Y. Lan *et al.*, Phys. Rev. Lett. **98**, 123602 (2007).
[19] R. Inoue *et al.*, Phys. Rev. A **74**, 053809 (2006).
[20] A. Vaziri *et al.*, Phys. Rev. Lett. **91**, 227902 (2003).
[21] Y.-A. Chen *et al.*, arXiv:0705.1256.
[22] D. A. Braje *et al.*, Phys. Rev. Lett. **93**, 183601 (2004).
[23] P. Kwiat *et al.*, Phys. Rev. Lett. **75**, 4337 (1995).
[24] J. F. Clauser, M. Horne, A. Shimony, and R. A. Holt, Phys. Rev. Lett. **23**, 880 (1969).
[25] D. M. Harber *et al.*, Phys. Rev. A **66**, 053616 (2002).